Jan Chleboun; Judita Runcziková; Pavel Krejčí
The impact of uncertain parameters on ratchetting trends in hypoplasticity

In: Jan Chleboun and Pavel Kůs and Jan Papež and Miroslav Rozložník and Karel Segeth and Jakub Šístek (eds.): Programs and Algorithms of Numerical Mathematics, Proceedings of Seminar. Jablonec nad Nisou, June 19-24, 2022. Institute of Mathematics CAS, Prague, 2023. pp. 37–46.

Persistent URL: http://dml.cz/dmlcz/703186

Programs and Algorithms of Numerical Mathematics 21
J. Chleboun, P. Kůs, J. Papež, M. Rozložník, K. Segeth, J. Šístek (Eds.)
Institute of Mathematics CAS, Prague 2023

THE IMPACT OF UNCERTAIN PARAMETERS ON RATCHETTING TRENDS IN HYPOPLASTICITY

Jan Chleboun, Judita Runcziková, Pavel Krejčí

Faculty of Civil Engineering, Czech Technical University in Prague
Thákurova 7, 166 29 Prague 6, Czech Republic
jan.chleboun@cvut.cz, judita.runczikova@fsv.cvut.cz, pavel.krejci@cvut.cz

Abstract: Perturbed parameters are considered in a hypoplastic model of granular materials. For fixed parameters, the model response to a periodic stress loading and unloading converges to a limit state of strain. The focus of this contribution is the assessment of the change in the limit strain caused by varying model parameters.

Keywords: granular material, hypoplasticity, ratchetting, uncertain parameters

MSC: 65Z05, 74C15, 74H40, 90C70

1. Introduction

In this contribution, the hypoplastic model [6] of granular materials is considered together with uncertain input parameters. The focus is concentrated on the influence the uncertainty in inputs has on the limit state of ratchetting. The limit state is, of course, determined only approximately through a numerical modeling of a finite number of cyclic loading and unloading steps.

Let us imagine a cohesionless granular material such as soil, sand, or gravel. Its behavior is different from common solid materials and cannot be modeled by common models widely used in elasticity and plasticity. Various models of hypoplastic granular materials have been proposed, see, for instance, a micromechanical approach [1, 3], a macromechanical approach [4], or a survey in [2] or [6]. As already indicated, we will use the model presented in the paper [6] that is a continuation of [2], and both follow the hypoplastic concept proposed in [5].

Unlike in common elasticity models where a body is loaded by forces that, through a strain, produce a stress, loading by stress is considered and strain inferred in hypoplastic models. An effect called ratchetting is then observed. It can be briefly characterized as a behavior in which deformation accumulates due to cyclic mechanical stress. As a consequence, the hypoplastic material is made denser and more compacted than the material before cycles of loading and unloading. The material

DOI: 10.21136/panm.2022.04

in an initial state is looser and has a greater void ratio (imagine a pile of fluffy soil under a cyclic loading). The material response to the cyclic loading is more and more stable. Finally, a limit state both in the strain and the void ratio is reached. In the limit, the void ratio takes its minimum that is given by the parameter e_d in our model, see (9) in Section 2. Our contribution is concerned with an arising question: How strongly is the limit strain influenced by the uncertainty in parameters that enter the model?

2. The hypoplastic model

The model whose response will be investigated is introduced in this section. We follow [6] but make the presentation significantly condensed. The reader can also get an idea of the model in [2] where, however, the exposition is not as straightforward as in [6].

The model [6] in a general form is given by

$$\dot{\boldsymbol{\sigma}}(t) = c_1(t)\big(L(\boldsymbol{\sigma}(t)) : \dot{\boldsymbol{\varepsilon}} + f(t)N(\boldsymbol{\sigma}(t))\|\dot{\boldsymbol{\varepsilon}}(t)\|\big), \tag{1}$$

where $\boldsymbol{\sigma}$ is the stress tensor, $\boldsymbol{\varepsilon}$ is the strain tensor, $c_1(t)$ and $f(t)$ are "time" dependent quantities, see (6) and (9), and $L(\boldsymbol{\sigma}(t))$ and $N(\boldsymbol{\sigma}(t))$ are tensors, see the next paragraph. The canonical scalar product is denoted by : and the dot stands for the derivative with respect to t, a time-like parameter on which the evolution of the loading process depends. Since a stress-controlled loading is considered, the stress $\boldsymbol{\sigma}(t)$ is given and the strain $\boldsymbol{\varepsilon}(t)$ is to be determined.

Let us particularize (1) in terms of matrices and scalar functions. The loading is specified as proportional to a given 3×3 symmetric matrix $\mathbf{S} = (s_{ij})_{i,j=1,2,3}$, that is, $\boldsymbol{\sigma}(t) = \sigma(t)\mathbf{S}$, where $\sigma : [b, b+T] \to (0, \infty)$ is a given monotone scalar function defined on an interval $[b, b+T]$ of the length T. The proportional loading or unloading is determined by the increasing or decreasing function σ, respectively.

Let us consider matrices $\mathbf{A}, \mathbf{B} \in \mathbb{R}^{3\times3}$, and introduce

$$\langle \mathbf{A}, \mathbf{B} \rangle = \mathbf{A} : \mathbf{B} = \mathrm{tr}(\mathbf{B}^{\mathrm{T}}\mathbf{A}) = \sum_{1\le j,k\le 3} a_{jk}b_{jk},$$

the Frobenius norm

$$\|\mathbf{A}\| = \langle \mathbf{A}, \mathbf{A} \rangle^{1/2}$$

as well as the identity matrix $\mathbf{I} \in \mathbb{R}^{3\times3}$.

Then the detailed form of the model (1) is as follows:

$$\dot{\sigma}(t)\mathbf{S} = c_1(t)\sigma(t)\left(a^2\langle \mathbf{S}, \mathbf{I} \rangle \dot{\boldsymbol{\varepsilon}}(t) + \frac{1}{\langle \mathbf{S}, \mathbf{I} \rangle}\langle \mathbf{S}, \dot{\boldsymbol{\varepsilon}}(t) \rangle \mathbf{S} + af(t)\|\dot{\boldsymbol{\varepsilon}}(t)\|\Big(2\mathbf{S} - \frac{1}{3}\langle \mathbf{S}, \mathbf{I} \rangle \mathbf{I}\Big)\right), \tag{2}$$

where $a > 0$ is a real parameter and f is a positive t-dependent function. Both quantities will be considered uncertain.

Let us assume $\dot{\sigma}(t) \neq 0$ and define a matrix-valued function $\mathbf{X}$ as well as a constant matrix $\mathbf{A}$

$$\mathbf{X}(t) = c_1(t)\frac{\sigma(t)}{\dot{\sigma}(t)}\dot{\boldsymbol{\varepsilon}}(t), \quad \mathbf{A} = \frac{\mathbf{Q}}{a^2 + \|\mathbf{Q}\|^2}, \tag{3}$$

where

$$\mathbf{Q} = \frac{\mathbf{S}}{\langle \mathbf{S}, \mathbf{I} \rangle}.$$

After some manipulation, see [6], the model (2) takes the following form

$$\mathbf{X}(t) = \mathbf{A} + af(t)\|\mathbf{X}\|\mathbf{B} \quad \text{for } \dot{\sigma}(t) > 0, \tag{4}$$
$$\mathbf{X}(t) = \mathbf{A} - af(t)\|\mathbf{X}\|\mathbf{B} \quad \text{for } \dot{\sigma}(t) < 0, \tag{5}$$

where

$$\mathbf{B} = \left(2 + \frac{1}{3a^2}\right)\mathbf{A} - \frac{1}{3a^2}\mathbf{I}, \quad f(t) = F(e(t)) = f_0\left(\frac{e(t) - e_d}{e_c - e_d}\right)^{\alpha}, \tag{6}$$

$e(t)$ is the void ratio and α, $e_c > e_d$ are positive constants that will be considered uncertain. Instead of f_0, a fixed value of 1 is used in [6]. Since we wish to perturb this value too, we introduce a parameter f_0 and consider it uncertain.

The mass balance equation implies a differential equation for the void ratio $e(t)$, namely,

$$\dot{e}(t) = (1 + e(t))\langle \dot{\boldsymbol{\varepsilon}}(t), \mathbf{I} \rangle. \tag{7}$$

Recall $\mathbf{X}(t) = c_1(t)\frac{\sigma(t)}{\dot{\sigma}(t)}\dot{\boldsymbol{\varepsilon}}(t)$, then, with the help of (7)

$$\langle \mathbf{X}(t), \mathbf{I} \rangle = c_1(t)\frac{\sigma(t)}{\dot{\sigma}(t)}\langle \dot{\boldsymbol{\varepsilon}}(t), \mathbf{I} \rangle = c_1(t)\frac{\sigma(t)}{\dot{\sigma}(t)}\frac{\dot{e}(t)}{1 + e(t)}. \tag{8}$$

Now, it is the right time to reveal that the function c_1 is also e dependent. Indeed,

$$c_1(t) = -\bar{c}(e(t) - e_d)^{-\beta}, \tag{9}$$

where the constants $\bar{c}$, β, and e_d will be considered uncertain but constrained by $0 < \bar{c}$, $1 \leq \beta$, and $e_d \in (0, 1)$. The meaning of (9) is that the material becomes rigid when $e(t)$ asymptotically converges (decreases) to e_d, see [6]. The parameter e_d represents the minimum void ratio of the granular material. It is one of the model input parameters and its physically realistic value can be obtained from measurements.

Remark 1: Unlike [6], where $1 < \beta$ is considered, we allow for $\beta = 1$ to represent uncertainty in β by a closed interval, see Section 3. The value $\beta = 1$ does not cause any singularity or discontinuity in the model behavior.

Let us choose a special sort of loading and unloading. In particular, let σ be continuous, piecewise exponential, and periodic with the period equal to $2T$. Moreover, let $\dfrac{\sigma(t)}{\dot\sigma(t)}$ be alternately equal to 1 if $\dot\sigma(t) > 0$, and -1 if $\dot\sigma(t) < 0$. This choice simplifies (8) and (3) to

$$\langle \mathbf{X}(t), \mathbf{I}\rangle = \eta c_1(t) \frac{\dot e(t)}{1+e(t)} \quad \text{and} \quad \mathbf{X}(t) = \eta c_1(t) \dot{\boldsymbol\varepsilon}(t), \tag{10}$$

where $\eta = 1$ if $\dot\sigma(t) > 0$, and $\eta = -1$ if $\dot\sigma(t) < 0$.

The left equality in (10) and the equalities (4)–(5) lead, after a clever manipulation, see [6, Section 4], to

$$\dot e(t) \frac{\widehat{c}_1(e(t))}{1+e(t)} \big(h(F(e(t))) - g(F(e(t)))\big) = 1 \text{ for } \dot\sigma > 0, \tag{11}$$

$$\dot e(t) \frac{\widehat{c}_1(e(t))}{1+e(t)} \big(h(F(e(t))) - g(F(e(t)))\big) = -1 \text{ for } \dot\sigma < 0, \tag{12}$$

where $\widehat{c}_1(e(t)) = c_1(t)$ and

$$h(f) = \frac{\langle \mathbf{A}, \mathbf{I}\rangle + \left(\langle \mathbf{B}, \mathbf{I}\rangle \langle \mathbf{A}, \mathbf{B}\rangle - \langle \mathbf{A}, \mathbf{I}\rangle \|\mathbf{B}\|^2\right) a^2 f^2}{\langle \mathbf{A}, \mathbf{I}\rangle^2 - \|\langle \mathbf{A}, \mathbf{I}\rangle \mathbf{B} - \langle \mathbf{B}, \mathbf{I}\rangle \mathbf{A}\|^2 a^2 f^2},$$

$$g(f) = \frac{\langle \mathbf{B}, \mathbf{I}\rangle \sqrt{\|\mathbf{A}\|^2 - a^2 f^2 \left(\|\mathbf{A}\|^2 \|\mathbf{B}\|^2 - \langle \mathbf{A}, \mathbf{B}\rangle^2\right)}\, af}{\langle \mathbf{A}, \mathbf{I}\rangle^2 - \|\langle \mathbf{A}, \mathbf{I}\rangle \mathbf{B} - \langle \mathbf{B}, \mathbf{I}\rangle \mathbf{A}\|^2 a^2 f^2}.$$

In (11)–(12), the functions $\widehat{c}_1$ and F are used instead of c_1 and f to emphasize the dependence on the function e, which is the unknown function in the ordinary differential equation (11)–(12).

The matrix function $\mathbf{X}(t)$ can be expressed through $\mathbf{A}$, $\mathbf{B}$, a, and $F(e(t))$, see [6, Section 4]. As a consequence, if $e(t)$ is known by solving (11)–(12), then $\mathbf{X}(t)$ is known too, and $\boldsymbol\varepsilon(t)$ can be determined from the right equality in (10).

Remark 2: If $\mathbf{S} = -\mathbf{I}$, then (4)–(5) represent the case of isotropic loading. A detailed analysis of this special case together with a convergence analysis is presented in [6, Sections 2 and 3].

Remark 3: Let the function σ that reduces (8) to (10) be defined as in [6, Section 2]. In detail, let σ_1 and σ_2 be two positive real numbers such that $\sigma_1 < \sigma_2$, let $T = \ln\sigma_2 - \ln\sigma_1$, and let $t_k = kT$ for $k = 0, 1, 2, \dots$. We define

$$\sigma(t) = \sigma_1 \mathrm{e}^{t - t_{2j}} \text{ for } t \in (t_{2j}, t_{2j+1}), \quad \sigma(t) = \sigma_2 \mathrm{e}^{t_{2j+1} - t} \text{ for } t \in (t_{2j+1}, t_{2j+2}). \tag{13}$$

3. Uncertain inputs

Before we elaborate on uncertain parameters, let us show the model response to crisp inputs. As in [6, Section 5], we fix $a = 0.4$, $e_c = 0.8$, $e_d = 0.4$, $f_0 = 1$, $\alpha = 0.1$,

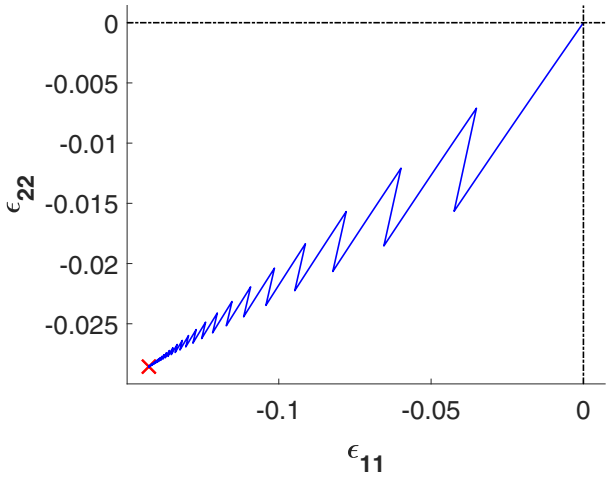

Figure 1: Ratchetting. The cross marks the numerical limit after 50 loading-unloading cycles. The strain evolution is fully characterized in the $\varepsilon_{11}\varepsilon_{22}$-plane because $\varepsilon_{22} = \varepsilon_{33}$.

$\bar{c} = 2$, $\beta = 1.03$, $\sigma_1 = 10$, and $\sigma_2 = 12$. The initial conditions are $e_0 = e(0) = 0.7$ and $\boldsymbol{\varepsilon}(0) = 0 \cdot \boldsymbol{I}$. Let the matrix $\mathbf{S}$ be diagonal with $s_{11} = -1.5$ and $s_{22} = s_{33} = -1$.

Let us focus on strain as the model monitored response. We have $\varepsilon_{22} = \varepsilon_{33}$ by virtue of the chosen values of $\mathbf{S}$. This feature allows for graphing the full strain evolution in the $\varepsilon_{11}\varepsilon_{22}$-plane in the course of 50 loading-unloading cycles, see Fig. 1. Although the loading and unloading are periodic, the strain cycles are not. As they converge to an equilibrium, we observe a shift in their cycles accompanied by a decreasing amplitude. This phenomenon is called ratchet(t)ing, see, for example, [1, 3].

Let us define the quantity of interest (QoI) as the numerical limit (after 100 cycles) of the strain in the $\varepsilon_{11}\varepsilon_{22}$-plane, see Fig. 1. We will investigate the sensitivity of the QoI with respect to eight parameters, namely, a, f_0, e_c, e_d, α, $\bar{c}$, β, and the initial condition e_0. The initial condition $\boldsymbol{\varepsilon}(0) = 0 \cdot \mathbf{I}$ and the loading parameters σ_1 and σ_2, see (13), remain fixed.

Let us make the listed parameters uncertain. To this end, we define the vector $u = (0.75, 0.8, 0.85, 0.9, 0.95, 1,\ 1.05, 1.1, 1.15, 1.20, 1.25)$ and vectors $a^{\text{unc}} = au$, $f_0^{\text{unc}} = f_0 u$, $e_c^{\text{unc}} = e_c u$, etc., where the nominal values from the first paragraph of this section are used in a, f_0, e_c, etc. In other words, the nominal values will be decreased or increased in 5% steps up to 25%.

The only exception is β, for which we define $\beta^{\text{unc}} = 0.55 + 0.6u$ to allow for a significant amount of uncertainty covering also the nominal value of 1.03.

Our goal is to record the QoI (the limit of the strain) if uncertainty is considered in one parameter and the other parameters remain fixed at their nominal values.

For $s_{11} = -1.5$ and $s_{22} = s_{33} = -1$, the computation shows that the influence of the uncertainty in the parameters can be divided into two groups. One group is

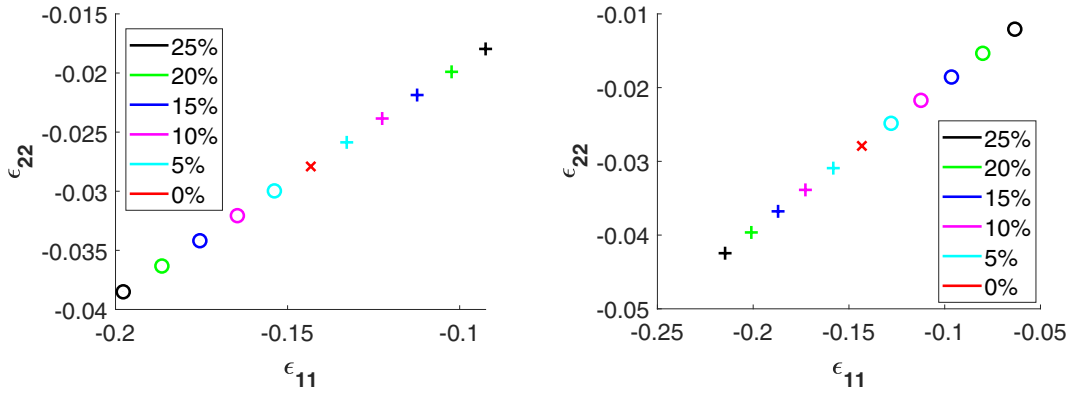

Figure 2: Response to the uncertainty in e_d (left) and e_0 (right). The symbol $\circ$ at the extreme position corresponds to the -25% change of the parameter nominal value, the symbol $+$ at the extreme position corresponds to the $+25\%$ change of the parameter nominal value, the symbol $\times$ marks the QoI if the parameter has its nominal value.

formed by f_0^{unc}, e_c^{unc}, α^{unc}, $\bar{c}^{\text{unc}}$, β^{unc} and the other by a^{unc}, e_d^{unc}, e_0^{unc}. In the former group, the uncertain input causes a response (in ε_{11} as well as ε_{22}) within 0.2%–5% of the response to the nominal values. The response is significantly stronger in the latter group and reaches 30%–60% as we can see in Fig. 2. Regarding a, the responses are located on a segment-like curve that starts at $(-0.18, -0.1)$ for -25% and ends at $(-0.125, -0.036)$ for $+25\%$.

Let us make the anisotropy stronger by setting $s_{11} = -2.0$ and $s_{22} = s_{33} = -1$. The basic division into two groups of parameters has been preserved though the response to $\bar{c}^{\text{unc}}$ has increased to $\pm 10\%$ of the reference value in ε_{22}, for instance. The range of the response to a^{unc} is larger and comprises both positive and negative values, that is, even the sign of the ε_{22} strain component is uncertain if sufficient amount of uncertainty is present in a, see Fig. 3. The responses to e_d^{unc} and e_0^{unc} are quite similar, only the latter is depicted in Fig. 3.

Since, as we observe, the anisotropy of $\boldsymbol{\sigma}$ has a strong influence on the range spread of QoI, we also investigate the model response to uncertainty in s_{11} with $s_{22} = s_{33}$ fixed to -1. We choose $s_{11} = -2$ as the nominal value that will be perturbed up to $\pm 25\%$. Fig. 4 shows the model responses.

4. Observations and comments

In Fig. 4 (right), we observe that the response of $\varepsilon_{22} = \varepsilon_{33}$ is close to zero if $s_{11} = -1.8$ or $s_{11} = -1.9$. As a consequence, a relatively small perturbation can cause a sign change. Negative strain means compression (in the corresponding direction), whereas positive strain means expansion. The latter phenomenon appears if the **S**-anisotropy is strong enough to make the material compressed in the 1-direction and (with a smaller magnitude) expanded in the 2- and 3-direction. This is also il-

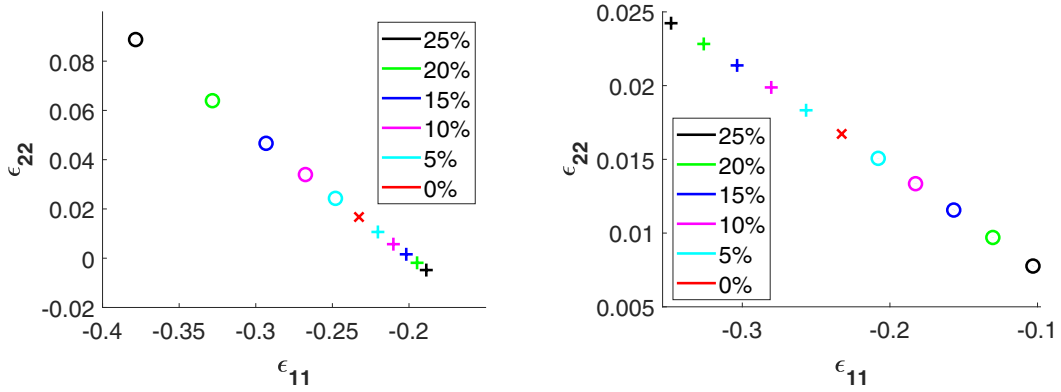

Figure 3: Response to the uncertainty in a (left) and e_0 (right). The symbol $\circ$ at the extreme position corresponds to the -25% change of the parameter nominal value, the symbol $+$ at the extreme position corresponds to the $+25\%$ change of the parameter nominal value, the symbol $\times$ marks the QoI if the parameter has its nominal value.

lustrated by Fig. 2 (right) and Fig. 3 (right). In the former case ($s_{11} = -1.5$), compression is observed in the 2-direction, whereas expansion comes in the latter case where $s_{11} = -2$.

Nevertheless, the computation shows that the void ratio $e(t)$ tends to its limit e_d (not depicted), that is, that the material is compacted for $s_{11} \in [-2.5, -1.5]$.

We also observe that changes of parameter values can result in an amplified or attenuated total effect. The latter is illustrated by Fig. 3, where an increase in a decreases the magnitude of both ε_{11} and ε_{22}, but an increase in e_0 has an opposite effect.

In some cases, a parameter-to-response mapping is nonlinear, see, for instance, Fig. 3 (left), where the negative perturbations have significantly stronger effect than the positive perturbations.

Although most of the graphs show points $[\varepsilon_{11}, \varepsilon_{22}]$ distributed along a line, a closer inspection would reveal a slight nonlinearity. A stronger nonlinear behaviour is depicted in Fig. 4 (left). The question arises whether the observed tendency to form an almost linear pattern has a deep reason rooted in the setting of the model, or whether it is simply the consequence of a limited amount of uncertainty that prevents nonlinearities to be fully developed; see Fig. 4 (left) where the circles form a linear pattern for $\beta \in [1, 1.12]$ that becomes curved if β belongs to $[1.15, 1.3]$, that is, to the interval relatively distant from the nominal value $\beta = 1.03$.

Readers familiar with fuzzy sets certainly noticed that relevant membership functions can be constructed on the basis of Fig. 2–4. Indeed, the ε_{11}-distance between two marks determined by the same (except for the sign) perturbation percent is the length of an α-cut of a membership function representing the fuzziness of ε_{11} induced by the fuzziness of one input parameter. Similarly for ε_{22}. However, a more elaborate approach is necessary if a fuzzy set based on Fig. 4 (left) is to be inferred.

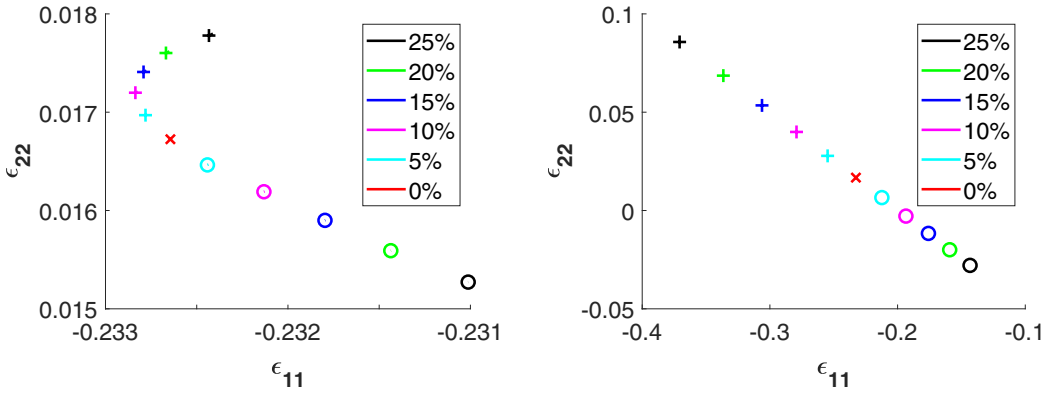

Figure 4: Left: Response to the uncertainty in β. The symbol $\circ$ at the extreme position corresponds to $\beta = 1$, whereas the symbol $+$ at the extreme position marks the response to $\beta = 1.3$; the β-step is equal to 0.03. Right: Response to the uncertainty in s_{11}. The symbol $\circ$ at the extreme position corresponds to the response to $s_{11} = -1.5$, whereas the symbol $+$ at the extreme position marks the response to $s_{11} = -2.5$; the s_{11}-step is equal to 0.1.

All the calculations were performed in the MATLAB® environment.

Acknowledgments

The research of the first author was supported by the project Centre of Advanced Applied Sciences (CAAS) with the number: CZ.02.1.01/0.0/0.0/16_019/0000778. CAAS is co-financed by the European Union. The first author is also grateful to Dr. Richard (Dick) Haas for fruitful discussions. The work of the second author was supported by the Grant Agency of the Czech Technical University in Prague, grant No. SGS22/005/OHK1/1T/11. The work of the third author was supported by the Czech Science Foundation, project No. 20-14736S. The research was also supported by the OeAD Scientific & Technological Cooperation (WTZ CZ 18/2020: "Hysteresis in Hypo-Plastic Models") financed by the Austrian Federal Ministry of Science, Research and Economy (BMWFW) and by the Czech Ministry of Education, Youth and Sports (MŠMT).

References

[1] Alonso-Marroquín, F., Mühlhaus, H.B., and Herrmann, H.J.: Micromechanical investigation of granular ratcheting using a discrete model of polygonal particles. Particuology **6** (2008), 390–403. URL https://www.sciencedirect.com/science/article/pii/S1674200108001430.

[2] Bauer, E. et al.: On proportional deformation paths in hypoplasticity. Acta Mechanica **231** (2020), 1603–1619. URL https://link.springer.com/article/10.1007/s00707-019-02597-3.

[3] Calvetti, F. and di Prisco, C.: Discrete numerical investigation of the ratcheting phenomenon in granular materials. Comptes Rendus Mécanique **338** (2010), 604–614. Micromechanics of granular materials, URL https://www.sciencedirect.com/science/article/pii/S1631072110001567.

[4] Karrech, A., Seibi, A., and Duhamel, D.: Finite element modelling of rate-dependent ratcheting in granular materials. Computers and Geotechnics **38** (2011), 105–112. URL https://www.sciencedirect.com/science/article/pii/S0266352X10001187.

[5] Kolymbas, D.: An outline of hypoplasticity. Arch. Appl. Mech. **61** (1991), 143–151. URL https://link.springer.com/article/10.1007/BF00788048.

[6] Krejčí, P., Monteiro, G.A., Runcziková, J., Bauer, E., and Kovtunenko, V.A.: Stress-controlled ratchetting in hypoplasticity (submitted to Acta Mechanica in October 2022).